FINE STRUCTURE OF SHOCK WAVES IN A PLASMA AND THE MECHANISM OF SATURATION OF ION-ACOUSTIC TURBULENCE

V. G. ESELEVICH, A. G. ES'KOV, R. Kh. KURTMULLAEV, and A. I. MALYUTIN

Nuclear Physics Institute, Siberian Division, U.S.S.R. Academy of Sciences

Submitted September 28, 1970

Zh. Eksp. Teor. Fiz. 60, 1658–1671 (May, 1971)

The results are presented of an investigation of the fine structure of transverse shock waves in a collisionless plasma at Mach numbers $M < 2.5$. The distribution of the magnetic field was measured with the aid of a special probe, which made it possible to obtain a resolution down to 0.1 mm, and the distributions of the other quantities on the front were determined from the H(x) profile with the aid of the mhd equations. On the basis of the experimental data, it is suggested that in the case of an initially isothermal plasma the ion-acoustic instability develops after preliminary heating of the electrons either as a result of Joule dissipation by the classical resistance, or as a result of two-stream instability. The distribution of the quantities in the turbulent region of the front agrees with the assumed linear (resonant) mechanism of the interaction of the phonons with the hot ions. At the same time, the experimental value of the parameter A, which characterizes the nonlinear interaction, differs from the predicted one by at least one order of magnitude.

INTRODUCTION

At present it can be regarded as established that the existence of collisionless shock waves in a plasma placed in a magnetic field is connected, in a wide range of parameters, with the phenomenon of anomalous resistance. Although the available experimental data have made it possible to conclude that the most probable cause of the anomalous resistance of the plasma is the development of ion-acoustic turbulence,[1-3] there is still no complete physical picture of the processes in the shock front. In particular, one of the most important questions remains open, namely that of the mechanism limiting the growth of the amplitude of the turbulent fluctuations. The equilibrium level of the fluctuations determines the effective frequency of the electron-ion collisions, and consequently the dissipative properties of the plasma and the structure of the shock front. We note that the question of the mechanism of saturation of ion sound lies beyond the scope of the problem of collisionless shock waves and is important in all cases when the processes in the plasma are accompanied by the development of ion-acoustic instability.

An exhaustive answer can be obtained by measuring the turbulence spectrum $E(\omega, k)$. The first measurements in the long-wave part of the spectrum were based on the Raman scattering of radio waves[4] or made with the aid of probes.[1,2] At present results are available on small-angle scattering of a laser beam[5] and on the Stark effect.[6] However, such important information as the form of Ohm's law, which characterizes the anomalous resistance of the plasma, can also be obtained by investigating details of the behavior inside the front of such quantities as the magnetic field or the potential. To this end it is necessary to obtain sufficiently high spatial and temporal resolution in the registration of the indicated quantities. As will be shown below, none of the methods used to date are applicable from this point of view, and therefore we used in the present investigation an improved probe procedure, which made it possible to improve considerably the resolution compared with earlier methods (for example, compared with the usual loop-type magnetic probe).

In the analysis of the observed structure of the magnetic field we shall use a system of equations in the mhd approximation, describing the resistive shock front in the form given in the paper of Galeev and Sagdeev:[7]

$$\rho v = \text{const}, \quad J \equiv \rho v + p + H^2/8\pi = \text{const}, \quad L \equiv \frac{\gamma}{\gamma-1}\frac{p}{\rho} + \frac{v^2}{2} + \frac{HH_0}{4\pi\rho_0} = \text{const}, \quad vH = \frac{c^2}{4\pi\sigma_{\text{eff}}}\frac{dH}{dx} + \text{const}, \tag{1}$$

where $\rho = m_i n$ is the plasma density, v is the translational velocity of the ions in the wave system, $p = nT$ is the pressure, and σ_{eff} is the effective conductivity of the plasma.

For simplicity we introduce the dimensionless quantities

$$h = H/H_0 = 1 + \Delta H/H_0, \quad w = v/u = n_0/n, \quad \beta = 8\pi nT/H_0^2, \quad M = u\sqrt{4\pi n_0 m_i}/H_0.$$

From the first three equations, which are the laws of conservation of the mass flux, momentum density, and energy density, we can obtain the functions w(h) and β(h):

$$w = \frac{\gamma}{\gamma+1}\left(\frac{J}{\rho_0 u^2} - \frac{h^2}{2M^2}\right) + \left\{\left[\frac{\gamma}{\gamma+1}\left(\frac{J}{\rho_0 u^2} - \frac{h^2}{2M^2}\right)\right]^2 - \frac{2(\gamma-1)}{\gamma+1}\left(\frac{L}{u^2} - \frac{h}{M^2}\right)\right\}^{1/2} \tag{2}$$

$$\beta = \beta_0 + \Delta\beta = \beta_0 + 2M^2(1-w) - h^2 + 1, \tag{3}$$

and from the fourth equation of the system (1) we can determine the conductivity inside the front.

APPARATUS AND INITIAL CONDITIONS

The experiments were performed with the UN-4 apparatus.[1] The hydrogen plasma was produced in a cylindrical glass volume of 16 cm diameter and 100 cm

length with the aid of an induction discharge. The plasma density in the different regimes and its distribution over the volume were determined by the microwave-interferometry method.[8] Operating control over the initial concentration n_0 and the electron temperature T_{e0} was with the aid of a triple Langmuir probe.[9] The degree of ionization was approximately 50% at $n_0 \lesssim 5 \times 10^{13}$ cm^{-3} and reached 80–90% at $n_0 > 5 \times 10^{14}$ cm^{-3}. The initial electron temperature under typical regimes ranged from $T_{e0} = 0.5$ eV to $T_{e0} = 2$ eV. The ion temperature was not measured directly, but one could expect $T_{i0} \approx T_{e0}$, since the lifetime of the plasma up to the instant of generation of a shock wave, 3×10^{-5} sec, was much longer than the time of temperature relaxation, 5×10^{-7} sec (at $T_{e0} = 1$ eV and $n_0 \sim 10^{14}$ cm^{-3}). The quasistationary initial magnetic field H_0 was varied in the range 100–2000 Oe; the degree of inhomogeneity of H_0 in the region of registration of the shock wave did not exceed 2%,[10] and the characteristic variation time was 250 μsec. In accordance with the indicated initial conditions, the relative pressure $\beta_0 = 8\pi n_0 T_0 / H_0^2$ assumed values from 0.005 to 0.05.

The cylindrical shock wave was excited with the aid of a magnetic piston by discharging a capacitor into a surge turn of 30 cm width. The amplitude of the piston under typical conditions was 2–3 kOe, and its growth time was 400 nsec. The magnetic field of the piston and the initial field H_0 were parallel and had the same direction.

REGISTRATION SYSTEM

To obtain maximum spatial resolution in measurements of a magnetic field by a loop probe it is necessary that the characteristic dimension in the direction of propagation of the wave be small. However, a decrease of this dimension is limited by technical difficulties connected, for example, with the need for providing reliable electric insulation of the measuring circuit from the plasma. Therefore the presently attainable resolution 0.4–0.5 mm is probably the limit for probes of this type (see also [11]).

We propose in this paper a probe of new design, making it possible to improve greatly the resolution of the fine structure of the magnetic perturbations. In the case

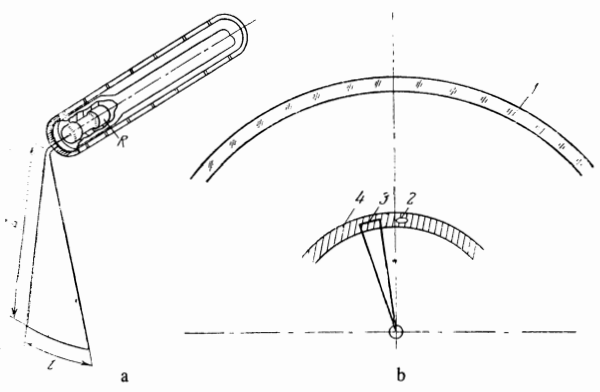

FIG. 1. Exterior view of the sector probe (a) and magnetic field registration scheme (b): 1–cylindrical volume, 2–loop-type magnetic probe, 3–sector probe, 4–wave front.

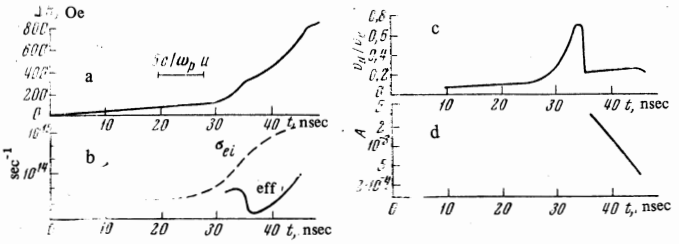

FIG. 2. Distribution of magnetic field (a), conductivity (b), the ratio v_d/v_e (c), and A (d) in wavefront. Hydrogen, $n_0 = 1.5 \times 10^{14}$ cm^{-3}, $H_0 = 700$ Oe, M = 2.

when the measured fields have axial symmetry, such a probe is a circuit made of thin insulated wire (0.1–0.2 mm) in the form of a sector of radius L = 20–40 mm and arc l = 3–10 mm (Fig. 1a). The vertex of the sector is placed on the axis of the plasma volume, so that the arc is "parallel" to the front of the wave (Fig. 1b). For the stationary case, the induced emf in the circuit is given by the expression

$$\mathscr{E} = \frac{1}{c}\frac{d\Phi}{dt} \approx \frac{1}{c} u \Delta H(t),$$

so that by measuring the wave velocity u it is possible to determine the absolute value of the magnetic field $H = H_0 + \Delta H(t)$ at the point with radius r = L.[1)] The aperture angle θ and the value of the resistance R were chosen such that the inductive reactance of the probe was much less than the load resistance. In the performed experiments, the angle θ ranged from 5 to 30°, and the resistance built into the probe ranged from 0 to 500 ohm.

Notice should be taken of the stringent requirements that are imposed on the manufacturing quality of probes of this type and on the accuracy of their placement in the working volume. Maximum resolution and the exact value of the amplitude can be obtained only if the arc of the sector probe is strictly "parallel" to the front, and the lateral components are radially directed. In this case the resolving power is limited by two factors: the diameter of the wire of which the probe circuit is made (b) and the frequency band of the measuring channel. (The apparatus used in the present investigation had an attenuation of 3–6 dB at f_0 = 1000 MHz.) Thus, no distortion will occur in the registration of magnetic-perturbation details having spatial dimensions larger than d and u/f_0. In our case the limiting resolution reached 10^{-2} cm, providing an appreciable gain over the probes used heretofore.[1, 12, 13]

To measure the potential of the electric field in the wave, we used electric probes with a temporal resolution up to several nanoseconds (corresponding to a spatial resolution up to 10^{-2} cm). The construction of the probe and a simple outline of the operating theory of such probes are given in [14].

[1)] Simultaneous measurement of the magnetic perturbations by loop and sector probes made it possible to obtain such quantities as the distribution of the phase velocity of the magnetic perturbations (i.e., the degree of stationarity of the wave), the plasma pressure on the piston, the exact value of the amplitude of the reflected wave, etc.

FINE STRUCTURE OF THE FRONT

1. The question of the fine structure of the front of a transverse shock wave arises in connection with attempts to construct a detailed picture of the occurrence and dynamics of the development of the anomalous resistance of the plasma in the transition layer, inasmuch as there is a unique inverse connection between the spectrum of the turbulence excited in the front and the shock-wave structure. Nor is it known which processes precede the development of the ion-acoustic turbulence in an initially isothermal plasma. To investigate these questions we used a method based on measurement of the detailed distributions of the values of H and φ inside the front.

2. Figures 2a, 5a, 6a, and 7a show typical oscillograms of the magnetic perturbations, as obtained with the aid of the sector probe in a hydrogen plasma at different initial concentrations. The first interesting fact is that these oscillograms differ from the signals obtained in analogous regimes with the aid of loop probes having diameters on the order of 1–3 mm. First, we see that the profile of the magnetic field becomes steeper up to the very crest of the wave; the values of the derivatives of the magnetic field and of the drift velocity can in this case be 3–5 times larger than the mean values obtained for these quantities by reducing oscillograms from a loop probe.

The second feature is that under typical experimental conditions, one observes on the magnetic-field profile a more or less clearly pronounced kink (Fig. 2a). It has been observed that the relative position of this kink depends on the initial conditions, for example, it shifts towards the crest of the wave when the initial concentration is increased.

It must be ascertained, however, whether the indicated effects are due to operating singularities of the sector probe. For example, the continuous increase of the slope of the registered signal could, generally speaking, be a consequence of the nonstationary character of the process if the phase velocity of the perturbation of the magnetic field increases continuously with increasing depth in the interior of the transition layer.

To answer this question, simultaneous measurements were made of the magnetic field with sector and loop microprobes with resolving power 0.5 mm. Figure 3 shows the derivative of the magnetic field registered with the aid of a microprobe in a regime close to that indicated in Fig. 2 (the front terminates at the instant of time $t \approx 23$ nsec). One can see clearly the two-component structure of the signal, i.e., in the case of relatively low concentration the readings of both probes practically coincide, thus indicating that the plasma

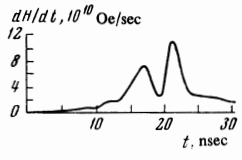

FIG. 3. Magnetic-field derivative registered with the aid of a loop microprobe with dimensions 3 × 0.4 mm. (Termination of the front at t = 23 nsec). Hydrogen, $n_0 = 1.3 \times 10^{14}$ cm^{-3}, $H_0 = 550$ Oe.

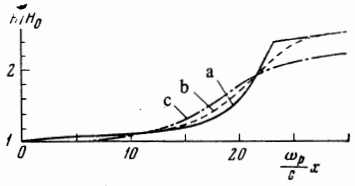

FIG. 4. Signal from sector probe (a) averaged over the dimension of a loop probe of 1.8 mm diameter (b) ($n_0 = 6.5 \times 10^{14}$ cm^{-3}, M = 2.4). Curve c—profile of H(x) given in [12,13] ($n_0 = 6.2 \times 10^{14}$ cm^{-3}, M = 2.5.

flow in the transition layer is stationary. When the initial concentration is increased by 4–6 times (i.e., when the absolute dimension of the front Δ is decreased by a factor 2–2.5) the microprobe no longer resolves the indicated details, whereas the signal from the sector probe remains qualitatively unchanged. We see therefore that for a correct measurement of the magnetic field in the wave one cannot use probes with a resolution worse than $0.1\,\Delta$. (In the regime with $n_0 = 10^{14}$ cm^{-3} this requirement was satisfied: $\Delta \sim 5$ mm and the microprobe resolution is 0.5 mm). It is now obvious that the previously obtained[1, 3, 13, 15] profile of the magnetic field in the shock wave is distorted to one degree of another. The distortion is the largest in the case of a hydrogen plasma at Mach numbers $M < 3$ and $n_0 > 10^{14}$–2×10^{14} cm^{-3}.

It can be clearly verified that this distortion is due to averaging of the magnetic field over the dimension of the probe loop. Figure 4 shows the signal from the sector probe (a) under the conditions M = 2.4 and $n_0 = 6.5 \times 10^{14}$ cm^{-3}, as well as its transformed appearance after averaging over the probe loop dimension D = 1.8 mm (b). In [3, 11, 12], where the loop diameter was only 0.6 of the front width, the distortions of the profiles should be appreciable. Moreover, when the magnetic-probe signals given in the cited papers are compared with the readings of the sector probe (Fig. 4c), it can be noted that the difference between them cannot be attributed only to averaging over the loop dimension D = 0.9 mm. It can be assumed that the reason lies in the design of the probe. For example, since the loop is placed in the tube, the averaging is over a dimension equal, in the extreme case, to the external diameter of the tube. Moreover, in this case the signal can broaden and contract additionally because of the finite time of diffusion of the magnetic field from the plasma into the tube and partly because of the diamagnetic effect, as was demonstrated in [16]. Favoring these assumptions is also the distribution H(x) itself, which, unlike the distribution of the potential, does not have a clearly pronounced crest. A strong distortion of the measured magnetic field may possibly be another reason why the normalized magnetic profile lags the potential profile in the cited papers.

3. The front width is usually defined by

$$\Delta = (H_2 - H_0) \Big/ \left.\frac{dH}{dx}\right|_{max},$$

where H_2 is the magnetic field behind the wave and $dH/dx|_{max}$ is the maximum value of the derivative in the transition layer (see, for example, Fig. 4b). However, an examination of the signal from the sector probe (Fig. 4a) offers evidence that such a definition is arbitrary.

Paul et al.[12, 13] define the front width as the characteristic width of the potential profile. In this case the uncertainty is automatically transferred to the concept of the potential-front width, but there is also a more serious objection to such a definition: since the processes in the resistive front are due to diffusion of the magnetic field, the width of the front should be determined from the profile of H. In addition, the potential profile at M = 3–5 differs significantly from the profile of the magnetic field.[14]

Returning to Fig. 2, we see that the front has two characteristic points corresponding to the kink of the magnetic field and to the crest of the wave. The possibility of using these points to determine the width of the front will be considered below.

DETERMINATION OF THE PLASMA PARAMETERS INSIDE THE SHOCK-WAVE FRONT

1. The experiments of [1, 3, 16] have demonstrated that at $M < 2.5–3$ the total pressure behind the front of the resistive wave is $p = n(T_e + T_i) \approx nT_e$, and in the system (1) we shall therefore neglect the ion pressure compared with the electron pressure also in the interior of the front ($\beta = \beta_e$). We are interested in the distribution of the quantity v_d/v_e over the front (here $v_d = (c/4\pi e)dH/dx$ is the drift velocity and $v_e = \sqrt{T_e/M_e}$ is the thermal velocity of the electrons), and also in the distribution of T_e/T_i. The ratio T_e/T_i in the initial section of the transition layer (ahead of the kink of H) will be calculated by assuming the ion temperature to be equal to the initial temperature. We shall see subsequently that this assumption is valid in a wide range of initial parameters.

2. Figures 2b and 2c show the distributions obtained in this manner for the quantities σ_{eff}, σ_{ei}, and v_d/v_e, corresponding to the experimental variation of the magnetic field in the transition layer (Fig. 2a). Here $\sigma_{ei} \sim T_e^{3/2}$ is the classical conductivity due to the electron-ion collisions. It is seen from Fig. 2b that immediately behind the kink of the magnetic field there is observed a strong difference between σ_{eff} and σ_{ei}. There is an equally strong drop in the drift velocity of the electrons v_d (Fig. 2c). This means that the region of anomalous resistance begins behind the kink. We shall henceforth call this the turbulent region. We shall consider it in greater detail in the next section, and turn at present to the region of the front preceding the development of the turbulent resistance. One can expect the distribution of all the quantities in this region to be determined by the classical conductivity σ_{ei}, since the condition for the development of two-stream instability ($v_d > v_e$)[17] and one of the conditions for the buildup of ion-acoustic instability ($T_e \gg T_i$) are not satisfied.

We can now explain the observed structure of the magnetic field (Fig. 2a) in the following manner. Inasmuch as the initial plasma is isothermal, a certain time is required for the condition $T_e \gg T_i$ to become established in the plasma. The increase of the electron temperature is due to the Joule dissipation of the current in the front on the classical (Coulomb) resistance. With increasing h(x), the change of the parameters inside the transition layer occurs in such a way that the inequalities $v_d > c_s$ and $T_e \gg T_i$ ($c_s = \sqrt{T_e/m_i}$ is the speed of sound) are satisfied simultaneously at a certain instant of time, and then the plasma becomes unstable against the buildup of ion-acoustic oscillations. This instant correlates with the registered sharp drop of the effective conductivity. The front structure is subsequently determined by the value of the turbulent resistance. We note that in the investigated regimes the threshold value of the ratio T_e/T_i lies in the limits 5–7.

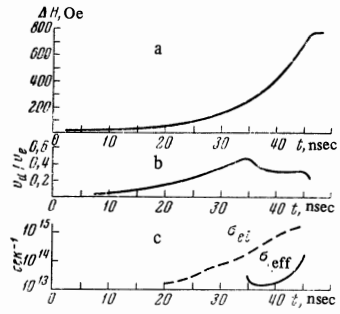

FIG. 5. Distribution of H, v_d/v_e, and σ in the front. Hydrogen, $n_0 = 10^{14}$ cm^{-3}, $H_0 = 925$ Oe, M = 1.65.

It follows from all the foregoing that our assumption $T_i \approx T_{io} \approx T_{eo}$ in the region of the front up to the kink is justified, since in classical heating the ion temperature increases more slowly than the electron temperature by a factor $(v_d/c_s)^2$.

The qualitative picture of the development of the process in the transition layer remains similar also for the case when the kink of the magnetic field is not so strongly pronounced as on the considered oscillogram (Fig. 2). It can be shown that the ratio of the derivatives dH/dx on the left and on the right of the kink depends on the initial conditions; for example, at fixed T_0 and β_0, the ratio of the derivatives decreases with decreasing Mach number, i.e., the kink becomes less distinct or disappears completely (Fig. 5a).

3. Let us consider now, for comparison, the distribution of the quantities in the transition layer under conditions of a relatively large initial concentration (Fig. 6, $n_0 = 6.5 \times 10^{14}$ cm^{-3}). As expected, in this case the kink of the magnetic field has shifted towards the

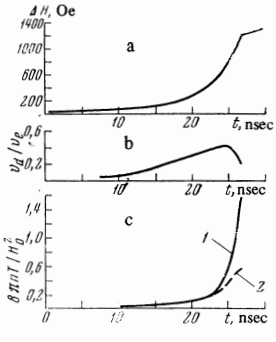

FIG. 6. Distribution of H, v_d/v_e, the relative pressure β (c, curve 1), and β_{ei} (c, curve 2). Hydrogen, $n_0 = 6.5 \times 10^{14}$ cm^{-3}, $H_0 = 900$ Oe, M = 2.4.

end of the front, i.e., the proposed region of pair collisions has broadened appreciably. Indeed, almost up to the very crest of the wave, the effective conductivity turns out to be close to σ_{ei}, and only at the end of the front is there a break in the drift velocity (Fig. 6b). The absence of turbulent resistance in the greater part of the transition layer is connected with the fact that the condition $T_e > 5T_i \approx 5T_{e0}$ is satisfied only when the instant $t \approx 25$ nsec is reached (Fig. 6c, curve 1). The condition for the buildup of the two-stream instability is likewise not satisfied, since $v_d < v_e$.

Although the front is formed in this case almost entirely at $\sigma_{eff} \approx \sigma_{ei}$, the contribution of the collisionless heating to the total heating of the plasma behind the wave is appreciable. In Fig. 6c, curve 1 represents the distribution of the total pressure, and curve 2 gives the contribution made to the heating by the Coulomb collisions. The last quantity was calculated from the formula.

$$p_{ei} = \frac{\gamma - 1}{u} \frac{1}{w^\gamma} \int_0^x \frac{j^2}{\sigma_{ei}} w^{\gamma-1} dx', \quad j = \frac{c}{4\pi} \frac{dH}{dx}. \qquad (4)$$

We note that with increasing n_0 the contribution of the classical heating in the turbulent region, Δp_{ei}, increases ($\Delta p_{ei}/\Delta p = 0.3$ as against 0.08 in the case of Fig. 2), and the width of the turbulent region decreases both in absolute magnitude (0.3 mm as against 3 mm) and with respect to the total scale of the perturbation. Therefore in a regime analogous to that shown in Fig. 6 it is very difficult to measure the quantities characterizing the turbulent state of the plasma, such as ν_{eff}, v_d/v_e, $E(k)$, and others.

Consequently, the study of the turbulent processes themselves in shock waves are best carried out at low initial concentrations ($n_0 \lesssim 10^{14}$ cm^{-3}), i.e., in those regimes where the region of the anomalous resistance is sufficiently large, and the turbulent processes reach a quasistationary phase in their development.

4. In order to visualize the structure of the shock wave at still higher concentration, we proceed as follows.

We obtain the distribution of the quantities H, n, T_e, and v_d/v_e inside the transition layer at $\sigma = \sigma_{ei} \sim T_e^{3/2}$ (in analogy with [18]). Calculation shows that in a wide range of values of the initial parameters H_0, T_0, and u there is satisfied the inequality $c_s < v_d < v_e$, provided only $n_0 > 5 \times 10^{13}$ cm^{-3}. As to the condition $T_e > (5-7)T_i$, the value of h(x) at which it is satisfied inside the front depends on β_0 and on the Mach number M; for example, when M = const and β_0 increases, the condition $T_e \approx 5\ T_i$ is satisfied closer to the end of the front and at a certain β_0 the electron temperature does not reach the level $5T_{e0}$ even behind the wave front. Consequently, the width of the turbulent region will decrease until it vanishes completely, and the profile of the wave will be determined to an ever-increasing degree by the paired collisions.

5. Thus, from the $\sigma(x)$ distribution we can construct the profile of the magnetic field in the front. If $\sigma \sim T_e^{3/2}$, then the spatial dimension of the transition layer Δ depends on the initial conditions in the form n_0^2/H_0^5 (at M = const), i.e., with decreasing n_0 the absolute value of Δ decreases and the drift velocity increases, with $v_d/v_e \sim H_0^4/n_0^{5/2}$.

The increase of the drift velocity with decreasing initial concentration n_0 makes it possible to explain the experimentally observed profiles of the magnetic field in the case of low concentrations.

Figure 7a shows the distribution of the magnetic field H(x) in the wave at $n_0 = 3.5 \times 10^{13}$ cm^{-3}; from this distribution it can be found, by the method described above, that $v_d \sim v_e$ in the forward narrow jump (Fig. 7b), and that the electron temperature increases by approximately five times. Consequently, in this case, too, the kink of the magnetic field is followed by a transition-layer region in which ion-acoustic turbulence probably develops, since v_d drops in this region to the level $0.2v_e$, a fact that can be attributed to the sharp decrease of the conductivity. The difference between this wave and those considered above (Figs. 2 and 4–6) lies in the method whereby the nonisothermy of the plasma is reached. In the cases shown in Figs. 2, 5, and 6, the preliminary "heating" of the electrons is due to paired Coulomb collisions, whereas in the presently considered case the natural "heating" mechanism is the Buneman instability, since the ratio v_d/v_e is limited to a value on the order of unity.[17]

The same sequence of development of instabilities in the collisionless front and a similar magnetic-field profile were established earlier in experiments with an argon plasma.[10]

At a still lower initial concentration, one can expect the time of passage of the plasma through the "Coulomb" section of the front to decrease to such an extent that the two-stream instability has no time to develop. This will occur if the time during which the condition $v_d \gtrsim v_e$ is satisfied inside the plasma turns out to be shorter than Λ/γ (γ is the increment of the two-stream instability and Λ is the Coulomb logarithm). Following this, the main mechanism blocking the further increase of the slope will be not dissipation but the dispersion of the magnetic sound, as a result of which a laminar oscillatory wave is formed. Such a transition was observed earlier in the investigation of shock waves in heavy-gas plasma at regimes where the resolution of the loop probes was sufficient.[10]

6. Returning to the determination of the front width, it should be noted that since the location of the "kink" of the magnetic field relative to the crest of the wave depends on the initial conditions, such a concept as the "width of the turbulent region of the front" is likewise not universal. A definition independent of the initial conditions can be introduced for the case of a "fully" turbulent transition layer (i.e., in the case $T_{e0} \gg T_{i0}$), if the width of the front is arbitrarily assumed to be the region in which

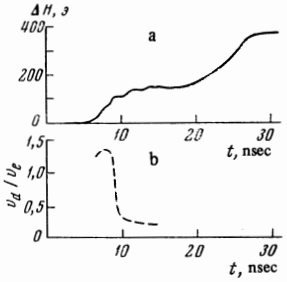

FIG. 7. Distribution of H and $v_d v/_e$ in the regime $n_0 = 3.5 \times 10^{13}$ cm^{-3}, $H_0 = 1000$ Oe, M = 1.3, hydrogen.

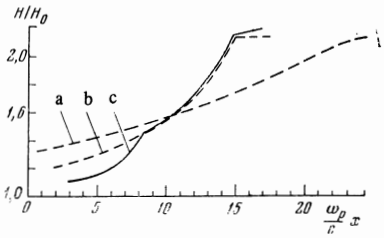

FIG. 8. Experimental profile of H(x) (c) and the profiles constructed under the assumption of a "linear" interaction at $v_d/v_e = 0.23$ (b) and a "nonlinear" interaction at $A = 10^{-2}$ (a).

the most significant change of H takes place, for example, from a value $H^* = H_0 + (H_2 - H_0)/e$ to $H = H_2$, where $e = 2.71$.

In the case when $T_{e0} = T_{i0}$, this definition can also be used if the "Coulomb" region of the front terminates at $H \ll H^*$. Under these assumptions, the width of the front for $M = 2$ is close to $(6-7)c/\omega_p$.

MECHANISM OF SATURATION OF ION-ACOUSTIC TURBULENCE IN THE SHOCK-WAVE FRONT

1. Thus, it follows from analysis of the structure of the magnetic field that satisfaction of the conditions $T_e > (5-7)T_i$ and $v_d > c_s$ is reached inside the front by one method or another, depending on the initial conditions, after which the plasma resistance increases strongly. It is precisely these conditions, as is well known, that are necessary for the development of ion-acoustic instability. At the present time there are two hypotheses, based on different assumptions with respect to the interaction of the phonons with the ions, and consequently determining two types of shock-wave structures.

According to the hypothesis of nonlinear damping of the ion-acoustic waves on ions,[7, 19] the effective collision frequency for the electrons is equal to

$$\nu_{\text{eff}} = A\omega_p \frac{v_d}{v_e}\frac{T_i}{T_e}, \quad \omega_p = \sqrt{\frac{4\pi ne^2}{m_e}}, \quad A = 10^{-2}. \tag{5}$$

In the case of linear interaction between the phonons and the high-energy ions,[20] we should have in the steady state

$$v_d / v_e \sim (m_e / m_i)^{1/4} \tag{6}$$

(for hydrogen, $(m_e/m_i)^{1/4} = 0.15$).

Knowing the distribution of the magnetic field inside the front, we can establish which of the indicated mechanisms is realized in experiment. There are several equivalent methods for this purpose. For example, it is possible to use Eq. (5) or (6) to obtain a theoretical profile of the magnetic field (at least in the turbulent region of the front), which is then compared with the experimental one. Figure 8 shows the profile of H(x) obtained with the aid of the sector probe at $M = 2$ (curve c) and the calculated profiles obtained by numerical integration assuming linear (b) and nonlinear (a) interactions of the phonons with the ions. As seen from the figure, the experimental profile coincides with the one constructed in the linear-interaction approximation when $v_d/v_e = 0.23$. At the same time, in order for the spatial scale of the profile (a) to approach the experimental one, it is necessary to take in (5) a coefficient $A \lesssim 10^{-3}$.[2)]

The other and more detailed analysis method consists in constructing distributions of the quantities v_d/v_e and A inside the transition layer. The calculation is based on the system of equations (1) with allowance for the ratio $T_e/T_i \approx v_d/c_s$. As seen from Figs. 2c and 2d, in the turbulent region the ratio v_d/v_e is practically constant and is close to the theoretical value $(m_e/m_i)^{1/4}$, whereas A is smaller by one order of magnitude than the theoretical value 10^{-2}, and what is more important, is not constant.

2. Similar results were obtained by two other independent methods. One of them is based on measurement of the distribution of the electric potential inside the front. If the potential $\varphi(x)$ is known, then we obtain from the equation of motion of the ions (neglecting the ion pressure)

$$v = u\sqrt{1 - 2e\varphi / m_i u^2}, \tag{7}$$

after which we find the distribution of all the remaining quantities that enter in the system (1). Measurement of the potential was carried out with the aid of probes of special design,[14] having a resolution down to a fraction of a millimeter (Fig. 9).

The second method is the method of local diamagnetic probes and makes it possible to obtain directly the distribution of the electron pressure nT_e over the front, in accordance with the relation

$$p_e = nT_e = (H_e^2 - H_i^2)/8\pi, \tag{8}$$

where $H_i \equiv H$ is the field in the plasma and H_e is the field inside a glass tube directed parallel to the force lines of the magnetic field. The distribution of the density and of the electron temperature can be calculated with the aid of the second equation of the system (1) in the following manner:

$$w = \frac{v}{u} = \frac{J}{\rho_0 u^2} - \frac{\beta + h^2}{2M^2} = 1 + \frac{1 - h_e^2}{2M^2}, \tag{9}$$

$$T_e = \frac{p_e}{n} = \frac{p}{n_0} w. \tag{10}$$

In this paper we used an improved procedure for measuring p_e (compared with that described in [16]). Nonetheless, when this method is used it is difficult to obtain a resolution better than 1 mm, and it is therefore used for measurements only in a sufficiently rarefied plasma ($n_0 \lesssim 10^{14}$ cm^{-3}).

Analyzing the experimental results obtained by these three methods and pertaining to the distribution of the quantities H, φ, v_d/v_e, and A inside the front, we can state that to explain the structure of the shock wave it is preferable to use the model based on the linear interaction between the ions and the phonons.

3. In conclusion, let us compare the described experimental data with the results of [3, 5, 11, 21]. In [3, 5, 11] the Thomson scattering of laser light was used to determine the electron temperature behind the wave

[2)] The weak dependence of the spatial scale on the coefficient A is connected with the fact that in the case of shock waves the quantities in the right-hand side of expression (5) depend on A. If we take this into account and rewrite ν_{eff} as a function of h (or x) only, then it turns out that $\nu_{\text{eff}} \propto A^{1/3}$. Therefore, we have also for the spatial scale $\Delta \propto A^{1/3}$

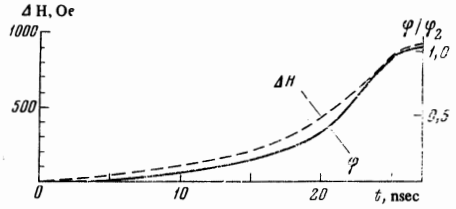

FIG. 9. Distribution of the magnetic field and of the potential in the transition layer, $n_0 = 1.8 \times 10^{14}$ cm^{-3}, $H_0 = 850$ Oe, M = 1.7, hydrogen.

front. The effective collision frequency averaged over the front was then estimated and compared with the quantity calculated from formula (5) at the average experimental parameters. Although the deviations of these quantities from one another amounted to a factor ranging from 0.2 to 0.6, the discrepancy between the theoretical value of A, namely 10^{-2}, and the experimental one turned out to be much larger, in view of the $\nu_{eff} \sim A^{1/3}$ dependence (see footnote 2). It is precisely to reconcile the measured and calculated values of ν_{eff} that it is necessary to choose A in the interval $10^{-4} < A < 2 \times 10^{-3}$.

Experiments on small-angle scattering of light[5, 13] cannot yet yield the distribution of ν_{eff} inside the front, since the region of the possible values of ν_{eff} is quite broad and depends on the assumed concrete form of the turbulence spectrum E(k). In addition, there is also a purely technical difficulty connected with decreasing the laser-beam diameter. (At the present time a beam of diameter 2 mm is used for a front thickness 1.5 mm.[5, 13].)

In [21] are given preliminary results on the measurement of the energy spectrum of ions in the front of a turbulent shock wave. The presence of high-energy ions containing the main fraction of the entire ion energy has been observed, and the temperature of the "hot" ions is close to T_e, something that can be explained within the framework of the model in which linear damping of the ion-acoustic waves by ions is assumed.

ESTIMATE OF THE ACCURACY OF THE RESULTS

The method of determining the distribution of the main quantities inside the transition layer from measurements of the magnetic perturbations, which is employed in the present work, makes use of the conservation laws in the shock wave. One of the most essential assumptions made by us is the condition $\Delta p_i \ll \Delta p_e$. This condition is satisfied with great accuracy in the Coulomb region of the front, but in the turbulent region, generally speaking, it is necessary to take into account the relation $dT_e/dT_i = v_d/c_s$,[7] which yields in accordance with Figs. 2c and 5b $T_i/T_e \sim 0.1$. Allowance for this correction, however, does not influence the qualitative course of the obtained distributions of v_d/v_e, A, and others, and the quantitative value changes in the range 10–20%. For example, the level of v_d/v_e increases by 1.05 times, the value of A decreases by a factor 1.1, and σ_{ei} by a factor 1.2. It is clear that the presence of this correction is not fundamental and can readily be taken into account.

Thus, the main error arises in measurements of the magnetic fields in the wave. As already mentioned, the errors in the determination of v_d from measurements made by ordinary probes with measuring-loop diameter D = 1–2 mm can reach 200–500% at the end of the front. The use of sector probes with a resolution down to 0.1–0.2 mm has made it possible to avoid an essential distortion of H(x) and by the same token eliminate the error in the measurement of the magnetic field.

In the calculation of the distributions of ν_{eff}, v_d/v_e and of other quantities by the method indicated above, there may, in the case of sufficiently large Mach numbers, be an increase in the errors connected with the presence of the electronic thermal conductivity, which is not taken into account in the system (1). It is easily shown that the ratio of the coefficients of turbulent thermal conductivity and the magnetic viscosity is close to 0.15 at M = 2, but reaches 0.3–0.35 already at M = 2.5.

Other measurement methods using the registration of $\varphi(x)$ or the simultaneous measurement of H_e and H_i are, generally speaking, less accurate: in the measurements of the potential, the limitations are due to the presence of a floating potential, while the diamagnetic-probe method has a resolution $\gtrsim 1$ mm. Their value lies in the fact that, being independent methods, they confirm qualitatively the main conclusions obtained with the aid of the sector probe.

The parameters of the initial plasma T_0, n_0, and H_0 are determined with accuracy 10–20%. These errors can result in random variations of the general level of the calculated quantity from one series of measurements to another. For example, the level of the "plateau" on the v_d/v_e distribution fluctuates between 0.22 and 0.33 for different cases. It should be noted that whereas at $v_d/v_e = 0.22$ the mean value of A is close to 10^{-3}, at $v_d/v_e = 0.33$ the value of A decreases to 3×10^{-4}. No noticeable dependence of the v_d/v_e level of the initial conditions (n_0, H_0, and β_0) was observed.

CONCLUSIONS

To obtain maximum spatial resolution in measurements of the magnetic field, we used a sector probe, which made it possible to observe the fundamental features of the fine structure of the shock front in a hydrogen plasma: first, the presence of two regions inside the front, separated by a more or less distinct kink of the magnetic field, and, second, an increase of the derivative on approaching the crest of the wave. On the basis of a study of the detailed distribution of the plasma parameters inside the front, it is shown that in the former region the electrons become heated because of Coulomb collisions (at $n_0 > 5 \times 10^{13}$ cm^{-3}) and that at low density ($n_0 < 5 \times 10^{13}$ cm^{-3}) another possible heating mechanism is two-stream instability. Thus, towards the end point of the first region both conditions necessary for the development of ion-acoustic instability, namely $v_d > c_s$ and $T_e > (5-7)T_i$, are satisfied.

In the turbulent region, the ratio v_d/v_e is almost constant and is close to the theoretical one $(m_e/m_i)^{1/4}$, whereas A is smaller by approximately one order of magnitude than the theoretical value $A = 10^{-2}$,[19] and is not constant. A comparison with the results published in other papers also leads to the conclusion that the

most probable mechanism for the damping of ion-acoustic oscillations in the front of the wave is their linear interaction with the ions.[20]

The authors are grateful to R. Z. Sagdeev for interest in the work.

[1] A. G. Es'kov, R. Kh. Kurtmullaev, A. I. Malyutin, V. I. Pil'skiĭ, and V. N. Semenov, Zh. Eksp. Teor. Fiz. **56**, 1480 (1969) [Sov. Phys-JETP **29**, 793 (1969)].

[2] S. G. Alikhanov, A. I. Alinovskiĭ, G. G. Dolgov-Savel'ev, V. G. Eselevich, R. Kh. Kurtmullaev, V. K. Malinovskiĭ, Yu. E. Nesterikhin, V. I. Pil'skiĭ, R. Z. Sagdeev, and V. N. Semenov, Third International Conference on Plasma Physics, Novosibirsk, 1968, paper 24/A-1.

[3] J. W. M. Paul, Collision-free Shocks in the Laboratory and Space, Proc. Study Group ESRIN, Frascati, June, 1969, p. 97.

[4] R. Kh. Kurtmullaev, V. L. Masalov, K. I. Mekler, and V. I. Pil'skiĭ, Paper at International Symposium on Shock Waves, Novosibirsk, 1967.

[5] J. W. M. Paul, C. C. Daughney, and L. S. Holmes, Collision-free Shocks in the Laboratory and Space, Proc. Study Group ESRIN, Frascati, June, 1969, p. 207.

[6] S. P. Zagorodnikov, G. E. Smolkin, E. A. Striganova and E. V. Sholin, ZhETF Pis. Red. **11**, 475 (1970) [JETP Lett. **11**, 323 (1970)].

[7] A. A. Galeev and R. Z. Sagdeev, Lectures on the Non-linear Theory of Plasma, Trieste, 1966.

[8] K. I. Mekler, Diplomate Thesis, Novosibirsk Electrical Engineering Institute, 1965.

[9] Sin Li Chen and T. Sekiguchi, J. Appl. Phys. **36**, 2363 (1965).

[10] R. Kh. Kurtmullaev, Dissertation, Nuclear Physics Institute, Novosibirsk, 1969.

[11] A. W. DeSilva et al., Conf. on Plasma Phys. and Controlled Nucl. Fusion Res., Novosibirsk, August, 1968 1968, paper CN-24/A-8.

[12] J. W. M. Paul, H. S. Holmes, M. J. Parkinson, and J. Sheffield, Nature **208**, 133 (1965).

[13] J. W. M. Paul, Culham Preprint CLM-P218, 1969.

[14] V. G. Eselevich, A. G. Es'kov, R. Kh. Kurtmullaev, and A. I. Malyutin, Zh. Eksp. Teor. Fiz. **60**, 2079 (1971) [Sov. Phys.-JETP **33**, No. 6 (1971)].

[15] S. P. Zagorodnikov, G. E. Smolkin, and E. V. Sholin, ibid. **52**, 1178 (1967) [**25**, 783 (1967)].

[16] R. Kh. Kurtmullaev, V. I. Pil'skiĭ, and V. N. Semenov, Zh. Tekh. Fiz. **40**, 1044 (1970) [Sov. Phys.-Tech. Phys. **15**, 804 (1970)].

[17] O. Buneman, Phys. Rev. **115**, 503 (1959).

[18] P. Jourdan, Plasma Phys. **11**, 57 (1969).

[19] R. Z. Sagdeev, Proc. Symp. Appl. Math., N.Y. 1965; AMS Providence, **18**, 281 (1967).

[20] G. G. Vekshteĭn and R. Z. Sagdeev, ZhETF Pis. Red. **11**, 297 (1970) [JETP Lett. **11**, 194 (1970)].

[21] N. I. Alinovskiĭ, A. T. Altyntsev, and N. A. Koshilev, Investigation of Heating of the Ionic Component of a Plasma by a Collisionless Shock Wave, Inst. Nucl. Phys. Preprint 5-71, Novosibirsk, 1970.

Translated by J. G. Adashko
183